Selective removal of divalent cations by polyelectrolyte multilayer nanofiltration membrane: Role of polyelectrolyte charge, ion size, and ionic strength

Submitted to

Journal of Membrane Science

January 20, 2017

Wei Cheng[1,2], Caihong Liu[1], Tiezheng Tong[3], Razi Epsztein[2], Meng Sun[2], Jun Ma[1]*, Menachem Elimelech[2]*

[1]*State Key Laboratory of Urban Water Resource and Environment, Harbin Institute of Technology, Harbin 150090, China*

[2]*Department of Chemical and Environmental Engineering, Yale University, New Haven, Connecticut 06520-8286, USA*

[3]*Department of Civil and Environmental Engineering, Colorado State University, Fort Collins, Colorado, 80523, USA*

*corresponding author
* E-mail: majun@hit.edu.cn (J.M), menachem.elimelech@yale.edu (M.E).
Tel: +86 451 86283010 (J.M), +1 203 432 2789 (M.E).
Fax: +86 451 86283010 (J.M), +1 203 432 4387 (M.E).

Abstract

We fabricated polyelectrolyte multilayer (PEM) nanofiltration (NF) membranes using a layer-by-layer (LbL) method for effective removal of scale-forming divalent cations (Mg^{2+}, Ca^{2+}, Sr^{2+}, and Ba^{2+}) from feedwaters with different salinities. Two polymers with opposite charges, polycation (poly(diallyldimethylammonium chloride), PDADMAC) and polyanion (poly(sodium 4-styrenesulfonate), PSS), were sequentially deposited on a commercial polyamide NF membrane to form a PEM. Compared to pristine and PSS-terminated membranes, PDADMAC-terminated membranes demonstrated much higher rejection of divalent cations and selectivity for sodium transport over divalent cations (Na^+/X^{2+}) due to a combination of both Donnan- and size-exclusion effects. A PDADMAC-terminated membrane with 5.5 bilayers exhibited 97% rejection of Mg^{2+} with selectivity (Na^+/Mg^{2+}) greater than 30. We attribute the order of cation rejection (Mg^{2+}> Ca^{2+}> Sr^{2+}> Ba^{2+}) to the ionic size effect, which governs both the hydration radius and hydration energy of the cations. The ionic strength (salinity) of the feed solution had a significant influence on both water flux and cation rejection of PEM membranes. In feed solutions with high ionic strength, abundant NaCl salt screened the charge of the polyelectrolytes and led to swelling of the multilayers, resulting in decreased selectivity (Na^+/X^{2+}) and increased water permeability. The fabricated PEM membranes can be potentially applied to the pretreatment of mild-salinity brackish waters to reduce membrane scaling in the main desalination stage.

Keywords: nanofiltration, polyelectrolyte multilayer, divalent cation removal, ionic strength, scaling control

Highlights

- A highly selective PEM membrane was fabricated via the LbL method.
- Mg^{2+}, Ca^{2+}, Sr^{2+}, and Ba^{2+} were used to explore the effect of ionic size on rejection.
- Impact of salinity on PEM membrane performance was investigated.
- PEM membranes can be applied to control scaling of mild-salinity brackish waters.

1. Introduction

Inorganic scaling is one of the major obstacles for efficient operation of membrane desalination and wastewater treatment systems [1-4]. Membrane scaling results in water flux decline and increases transmembrane pressure, thereby raising the cost of membrane desalination [5-7]. The most common inorganic scalants are formed by calcium- and magnesium-based precipitates such as calcium sulfate, calcium carbonate, and magnesium phosphate [8-10]. Other divalent cations (e.g., strontium and barium) are frequently found in shale gas produced wastewaters and may cause scaling in wastewater treatment operations [11-14]. Current strategies of scaling control are primarily based on the use of anti-scalants. However, using anti-scalants increases operational costs and induce organic and biological fouling [15-18]. Therefore, removing scale-forming divalent cations (X^{2+}) from the feedwater is a promising alternative for reducing scaling potential in water and wastewater treatment systems.

Nanofiltration (NF) is a competitive pretreatment approach to remove particularly divalent cations. In NF, Donnan (charge) exclusion and size (steric) exclusion are the main ion rejection mechanisms [19]. Therefore, due to their larger hydrated size and charge, divalent cations can be potentially rejected more favorably than monovalent cations by NF membranes [20]. High selectivity for the passage of monovalent cations over divalent cations (Na^+/X^{2+}) can help to maintain high water flux and energy efficiency. However, most commercial thin-film composite (TFC) NF membranes are negatively charged, weakening the Donnan exclusion of divalent cations by the membrane surface. For example, the rejections of $MgCl_2$ by two commercial TFC NF membranes, NF90 and NF270, were only about 70% at a pressure of 9 bar [21]. Also, these membranes present relatively high rejection of NaCl (85% and 40%, respectively), which results in low selectivity [22]. Therefore, developing NF membranes with a positive surface charge will favor the rejection of divalent cations (X^{2+}) over Na^+ and result in selective removal of scale-forming divalent cations from feedwaters.

Polyelectrolyte multilayer (PEM) nanofiltration membranes are fabricated by depositing polycations and polyanions alternately on a porous substrate, thus enabling control of membrane surface charge and permeability [23-25]. The type and deposition sequence of polyelectrolytes influence ion removal efficiency of PEM membranes. Importantly, the membrane surface charge is

determined mainly by the terminated polyelectrolyte layer (i.e. the top layer) [26]. Due to the Donnan-exclusion effect, PEM membranes terminated with polycations, such as Poly(diallyldimethylammonium chloride) (PDADMAC) and poly(allylamine hydrochloride) (PAH), favor divalent cations removal over monovalent cations [27]. Compared to PAH-terminated membranes, PDADMAC-terminated membranes often exhibit higher water flux due to their stronger swelling ability [28]. Generally, increasing the number of polyelectrolyte bilayers results in higher ion rejection and lower water permeability [26, 29, 30].

Feed solution ionic strength affects significantly the water and salt permeability of PEM membranes. For example, an increase of background ionic strength enhanced the permeability of PSS (poly(sodium 4-styrenesulfonate))/PAH multilayer capsules, as evidenced by the leakage of fluorescein dye through the capsule [31]. The authors explained the increased permeability of the multilayer membrane by the rearrangement of the polyelectrolyte segments as a response to charge screening (i.e., attraction of dissolved ions to opposite charges on the polyelectrolyte chain). It was also shown that the ionic strength of the feed solution has a nonlinear correlation with the permeability of ions through the PEM membrane due to attractive interaction between external ions and the charge of the polymer [32]. In another study involving forward osmosis, the high ionic strength of the draw solution enhanced the reverse solute flux of PEM membranes due to the increased compression of the electric double layer (EDL) [33].

The properties of the substrate (i.e., the underlying support for LbL assembly) also play a role in the performance of PEM membranes [34]. The most commonly used substrates to fabricate PEM NF membranes are porous inorganic alumina and polymeric microfiltration (MF) or ultrafiltration (UF) membranes [26, 35]. To strengthen the adsorption of polyelectrolytes, these substrates are often treated with O_3/UV or oxygen plasma to generate charged functional groups on the substrate surface [30, 36, 37]. Also, MF and UF porous substrates require a large number of polyelectrolyte bilayers to properly cover their large pores, resulting in extended fabrication time and decreased PEM stability. For example, seven PDADMAC/PSS bilayers on top of alumina substrate covered the underlying pores poorly, resulting in only 45% rejection of Mg^{2+} [28]. In contrast, TFC polyamide-based NF membranes possess negatively charged carboxyl groups [38] and require only a few bilayers to form a functional PEM membrane. Despite the potential of TFC membranes for use as substrates for LbL deposition, only a few studies have been reported on PEM membranes

utilizing such substrates [39-41].

In this study, we fabricated PEM NF membranes via layer-by-layer deposition on a negatively charged TFC NF membrane to selectively remove divalent cations from feed solutions with different ionic strengths. To understand the ion removal mechanism, we investigated the role of bilayer number and membrane surface charge in the rejection of four divalent cations with different ionic size (i.e., Mg^{2+}, Ca^{2+}, Sr^{2+}, and Ba^{2+}). By adjusting the concentration of NaCl to simulate various water sources (e.g., fresh water, brackish water, and sea water), we verified the significant influence of feed solution ionic strength on both cation rejection and water permeability of PEM membranes.

2. Materials and methods

2.1. Materials and chemicals

Poly(diallyldimethylammonium chloride) (PDADMAC; M_w = 400,000-500,000 Da, 20 wt% in water), poly(sodium 4-styrenesulfonate) (PSS; M_w = 70,000 Da), magnesium chloride hexahydrate ($MgCl_2 \cdot 6H_2O$), calcium chloride dihydrate ($CaCl_2 \cdot 2H_2O$), and strontium chloride hexahydrate ($SrCl_2 \cdot 6H_2O$) were purchased from Sigma-Aldrich. Sodium chloride (NaCl) and barium chloride dihydrate ($BaCl_2 \cdot 2H_2O$) were purchased from J. T. Baker. All the chemicals were ACS grade. Commercial TFC NF membrane (NFG) was provided by Synder Filtration. Deionized (DI) water was produced from a Milli-Q ultrapure water purification system (Millipore) and used for preparing solutions, compaction of membranes, and rinsing the NF system.

2.2. Polyelectrolyte multilayer membrane fabrication

The NFG membrane was chosen as the substrate for LbL deposition due to its relatively high water permeability (10.1-12.3 L m^{-2} h^{-1} bar^{-1}), low sodium rejection (10%), and large pore size (MWCO ~ 600-800 Da) (data provided by the manufacturer). Before the deposition of polyelectrolytes, the NFG membrane was immersed in 25% isopropanol for 30 minutes, followed by a thorough rinse with DI water. A home-made frame was used to ensure that the polyelectrolyte layers were only formed on the negatively charged active layer. PDADMAC and PSS were chosen as the polycation and polyanion, respectively. PDADMAC is a strong polycation that maintains a

permanent positive charge regardless of solution pH, whereas PSS is a strong polyanion with pKa at ~1 [42, 43]. Each polymer was dissolved in 0.2 M sodium chloride solution at a concentration of 0.1 g L^{-1}. The pH values of PDADMAC and PSS solutions were 5.5 and 5.8, respectively.

Figure 1 illustrates the fabrication procedure of the PEM membranes. In brief, the NFG membrane was dip-coated in 0.1 g L^{-1} PDADMAC solution for 30 minutes. After rinsing the membrane with 0.2 M NaCl solution (pH 5.7), the membrane was dip-coated in 0.1 g L^{-1} PSS solution to form the first bilayer. This deposition cycle was performed 1-5.5 times to fabricate PEM with 1-5.5 bilayers. In this study, membranes denoted as "0.5" bilayer were terminated with polycation (PDADMAC), whereas those denoted as integral bilayer were terminated with polyanion (PSS). After the deposition procedure, the PEM membranes were immersed in 15 wt% glycerol solution for four hours and dried overnight as suggested in the literature [27]. Before use, the membranes were rinsed with DI water thoroughly to remove glycerol.

Figure 1

2.3. Membrane characterization

The zeta potential of the membrane surface at different solution pH was measured by using a streaming potential analyzer with an asymmetric clamping cell (EKA, Brookhaven Instruments, Holtsville, NY); 1 mM KCl and 0.1 mM $KHCO_3$ were used as the background electrolytes. The detailed procedure used to calculate zeta potential from the measured streaming potential is described elsewhere [44, 45]. Eight measurements were performed for each pH and two coupons were measured independently for each membrane. The membrane surface morphology was characterized by scanning electron microscopy (SEM, Hitachi SU-70). Before measurement, the samples were dried overnight at ambient temperature and then coated with a thin film of iridium using a sputter coater (Denton Desk IV). The contact angle of the membrane was measured by the sessile drop method (OneAttension, Biolin scientific instrument) [46]. For each membrane coupon, eight contact angle measurements were conducted and the average value is presented.

2.4. Ion rejection and selectivity of PEM membranes

Four types of divalent cation (i.e., Mg^{2+}, Ca^{2+}, Sr^{2+}, and Ba^{2+}) were investigated. Ca^{2+} and Mg^{2+} are commonly found in brackish groundwater, while Sr^{2+} and Ba^{2+} are frequently detected in

shale gas-produced water [12, 13, 47-49]. A bench-scale cross-flow NF system was used to measure the water flux and cation rejection of PEM membranes. The dimension of the membrane cell was 77 mm × 26 mm × 3 mm and the surface area of the membrane coupon was 20.02 cm^2. All the measurements were conducted at 3.45 bar (50 psi) after six hours of membrane compaction with DI water at 4.14 bar (60 psi). Feed and permeate samples were collected one hour after the water flux stabilized in order to measure the rejection for each cation. Ion chromatography (IC; ICS-1000, Dionex, Sunnyvale, CA, USA) was used to measure the cation concentrations. The cross-flow velocity and temperature for all the experiments were maintained at 21.4 cm s^{-1} and 25 °C, respectively.

PEM membranes with different bilayer numbers and terminated polyelectrolytes were tested with a solution mixture containing 1 mM $CaCl_2$, 1 mM $MgCl_2$, and 5 mM NaCl. The removal efficiency and selectivity (Na^+/X^{2+}) of Ca^{2+} and Mg^{2+} were calculated to evaluate the effect of polyelectrolyte type and bilayer number on membrane performance. In addition, the influence of ionic size on cation rejection was investigated by using four salt solutions containing 1 mM divalent cations (Mg^{2+}, Ca^{2+}, Sr^{2+}, or Ba^{2+}). In order to analyze the effect of feed solution ionic strength, different concentrations of NaCl (in the range of 50 - 500 mM) were added to 5 mM $MgCl_2$. Finally, the removal of the above four divalent cations was investigated at high salinity (500 mM NaCl). The pH for all feed solutions used in this study was fixed at 6.0 ± 0.3.

The membrane selectivity for the passage of sodium (Na^+) over divalent cations (X^{2+}) was calculated using [24, 30]

$$Selectivity\ \frac{Na^+}{X^{2+}} = \frac{C_f(X^{2+})}{C_p(X^{2+})} \Big/ \frac{C_f(Na^+)}{C_p(Na^+)} = \frac{100-R_{Na+}}{100-R_{X2+}} \quad (1)$$

where C_f and C_p are the concentrations of cations in the feed solution and permeate, respectively; X^{2+} represents Mg^{2+}, Ca^{2+}, Sr^{2+}, or Ba^{2+}; and R is the rejection of each cation as calculated from

$$R = \left(1 - \frac{C_p}{C_f}\right) \times 100\% \quad (2)$$

3. Results and discussion

3.1. Effect of polyelectrolyte type and bilayer number on membrane properties and performance

3.1.1 PEM membranes characteristics

PDADMAC- and PSS-terminated PEM membranes with different bilayer numbers on top of the polyamide NF membrane (NFG) were fabricated using the LbL method. SEM images depicting the morphologies of the NFG and PEM membranes are presented in Fig. S1 and S2. The NFG substrate had a relatively smooth surface with small round structures randomly distributed. The PDADMAC-terminated PEM membranes were fully covered with a crumpled layer (Fig. S1). On the other hand, the PSS-terminated PEM membranes had no crumpled layers but rather round structures larger than those of the NFG substrate (Fig. S2). The terminating polyelectrolyte also altered membrane hydrophilicity as indicated by the measured water contact angles (Fig. S3). The PDADMAC-terminated membranes were more hydrophobic (water contact angle between 60° and 82°) than the PSS-terminated membranes and the pristine NFG membrane (water contact angle of about 40°) in agreement with previous studies [50, 51].

The zeta potential of the PEM membranes was measured at different solution pH (3-9) to explore the effect of terminating polyelectrolyte and bilayer number on membrane surface charge characteristics (Fig. 2). The pristine NFG membrane showed a negative surface charge above pH 4 due to the deprotonation of carboxyl groups on the polyamide membrane surface. The surface charge of PEM membranes was significantly affected by the type of capping polyelectrolytes. PDADMAC-terminated membranes showed less negative zeta potential than that of the NFG membrane at all solution pH investigated (Fig. 2A), with more positive values at increased bilayer number. Conversely, the PSS capping layer increased the negative surface charge compared to the NFG membrane (Fig. 2B), with more negative zeta potential observed for higher bilayer number. The zeta potential of the 5.5-bilayer membrane was identical to that of the 4.5-bilayer membrane, suggesting that the density of positive charge on the membrane surface reached a maximum after deposition of 4.5 bilayers. A similar phenomenon was observed for the PSS-terminated membranes after deposition of 4 bilayers.

Figure 2

3.1.2 Transport properties and separation performance of PEM membranes

The water permeability of PEM membranes was measured in a custom-built crossflow nanofiltration system operating at 3.45 bar (50 psi). Compared to the pristine NFG membrane, both

polycation- and polyanion-terminated PEM membranes exhibited reduced water permeability, with lower water permeability at higher bilayer number (Fig. 3A). This observation is attributed to the increased resistance to water permeation with an increase in the polyelectrolyte multilayer thickness [50]. The PDADMAC-terminated membranes (denoted as "0.5" bilayer) exhibited higher water permeability than the PSS-terminated membranes (denoted as an integer bilayer). We attribute this observation to the stronger swelling ability of the PDADMAC polymer than that of the PSS polymer, resulting in higher water mobility within the deposited PDADMAC multilayers [52, 53].

A feed solution containing 1 mM $CaCl_2$, 1 mM $MgCl_2$, and 5 mM NaCl was used to investigate the separation performance of the PEM membranes. The rejections of the three cations (i.e., Na^+, Ca^{2+}, and Mg^{2+}) are shown in Fig. 3B. The low rejections of both monovalent (4% for Na^+) and divalent (14.7% for Ca^{2+} and 15.7% for Mg^{2+}) cations by the pristine NFG membrane were due to its "loose" structure (MWCO ~ 600-800 Da). The PDADMAC-terminated membranes exhibited significantly improved rejection of Ca^{2+} and Mg^{2+}, yet maintained high permeation of Na^+. Modifying the NFG membrane with 5.5 bilayers of polyelectrolytes, for example, resulted in rejections of 94% and 98% for Ca^{2+} and Mg^{2+}, respectively, which were markedly higher than that for Na^+ (only 23%). Since the membranes with 4.5 and 5.5 bilayers had the same surface charge (Fig. 2A), the higher rejection of divalent cations observed for the 5.5 bilayer membrane are attributed to an increased size-exclusion effect with the addition of another bilayer. The high permeation of Na^+ and improved rejection of Ca^{2+} and Mg^{2+} resulted in an exceptional selectivity (characterized by the molar ratio Na^+/X^{2+} at the permeate) for the PDADMAC-terminated membranes (Fig. 3C). Increasing the bilayer number to 5.5, for example, enhanced the selectivity of the PDADMAC-terminated membranes up to a value of above 30.

In contrast to the results obtained with the PDADMAC-terminated membranes, divalent cations were not effectively removed by the PSS-terminated membranes (Fig. 3B and 3D). For example, the PSS-terminated membrane modified with five bilayers removed only 33% Ca^{2+} and 54% Mg^{2+} from the feed solution, resulting in low selectivity (Na^+/X^{2+}). Considering the electrostatic attraction between the PSS-terminated membrane surface and cations, the higher divalent cation rejection by the five bilayer PSS-terminated membrane compared to that with less bilayers can be ascribed to increased size-exclusion effect.

Figure 3

3.2. Selectivity of PEM membranes for different divalent cations (Mg^{2+}, Ca^{2+}, Ba^{2+}, and Sr^{2+})

Due to their scaling potential and common presence in freshwater, brackish water, or shale gas produced water, four divalent cations (i.e., Mg^{2+}, Ca^{2+}, Ba^{2+}, and Sr^{2+}) were chosen to evaluate the influence of ion size on the separation performance of PEM membranes. PEM membranes with 4.5 and 5.5 bilayers, which demonstrated high rejection for divalent cations (Fig. 3), were used in the following study.

Each divalent cation (1 mM) was mixed with NaCl (5 mM) individually to measure its rejection and selectivity (Na^+/X^{2+}) by the PEM membranes (Fig. 4A and 4B). The PDADMAC-terminated PEM membranes showed rejections higher than 80% for all the investigated divalent cations. A clear order of both rejection and selectivity (Ba^{2+}< Sr^{2+}< Ca^{2+}< Mg^{2+}) was found for the PEM membranes. The NFG membrane, with very "loose" structure, showed relatively low rejection for all cations and could not provide a clear trend of rejection or selectivity. The highest and lowest rejections observed for Mg^{2+} and Ba^{2+}, respectively, were in accordance with their hydrated radii difference (Table 1). While Sr^{2+} and Ca^{2+} have the same hydrated radius (0.412 nm) [54-57], the rejection of Ca^{2+} was slightly higher than that of Sr^{2+}. We attribute this observation to the different ionic charge densities and hydration energy of the two cations. Ca^{2+} has a higher ionic charge density than Sr^{2+} because of its smaller ionic radius (0.100 nm for Ca^{2+} *vs* 0.113 nm for Sr^{2+}) [58], leading to stronger electrostatic repulsion between Ca^{2+} and the positively charged PEM membrane surface [59, 60]. Also, Ca^{2+} with higher hydration energy (Table 1) holds the surrounding water molecules more strongly, and therefore undergoes lower dehydration than Sr^{2+} when entering the membrane pores [59, 61]. The removal efficiency and selectivity (Na^+/X^{2+}) for each divalent cation was investigated individually without NaCl (Fig. S4A and S4B). A similar removal efficiency and selectivity was observed as for the mixed solutions (Fig. 4), thus eliminating possible interactions between divalent cations and sodium chloride.

Figure 4

3.3. Impact of solution ionic strength on cation rejection and membrane permeability

Feedwaters simulating waters with various salinities (Table S1)— mildly brackish water,

257 moderately brackish water, heavily brackish water, and seawater—were prepared to investigate the
258 influence of ionic strength on salt rejection and water permeability of the fabricated PEM
259 membranes. The ionic strength of the feed solution was altered by varying the concentration of
260 NaCl from 50 mM to 500 mM. A constant concentration of $MgCl_2$ (5 mM) was added to all feed
261 solutions to provide divalent cations and mimic relatively high Mg^{2+} concentration in brackish water
262 [62].

263 Figure 5 shows that salt rejection by the commercial NFG membrane was independent of
264 feedwater salinity, whereas the rejection of Mg^{2+} declined substantially with the increase in solution
265 ionic strength for the PEM membranes. For example, the rejection of Mg^{2+} by the 4.5 bilayer
266 membrane decreased from 60% to 20% when NaCl concentration increased from 50 mM to 500
267 mM. We attribute the decrease in rejection at higher ionic strength to the screening of the positive
268 charge of PDADMAC by Cl^- anions, thereby weakening the Donnan exclusion effect and reducing
269 Mg^{2+} rejection [63].

270 **Figure 5**

271 The rejection of the other divalent cations (i.e., Ba^{2+}, Sr^{2+}, and Ca^{2+}) by the NFG and PEM
272 membranes was also tested under low (Figure 6A) and high (Figure 6B) ionic strength. In the
273 absence of NaCl, all the divalent cations showed high rejection of above 65% and 80% for the 4.5
274 and 5.5 bilayer PEM membrane, respectively. In the presence of 500 mM NaCl, however, the
275 rejection of all the divalent cations (at 5 mM) by the PEM membranes was significantly lower than
276 that without NaCl due to charge screening effect. For example, the rejection of Mg^{2+} dropped from
277 ~ 90% to ~ 20% for the 5.5 bilayer PEM membrane after the addition of 500 mM NaCl.

278 The water flux of the NFG and PEM membranes was affected by the increase in solution ionic
279 strength in different ways (Figure 6C). At high ionic strength, the water flux of the NFG membrane
280 was reduced by 20% due to the increase of feed osmotic pressure. In contrast, for the PEM
281 membranes, high ionic strength resulted in the increase of water flux by 30% and 50% for 4.5 and
282 5.5 bilayer PEM membranes, respectively, likely due to the swelling of the polyelectrolytes.
283 Increased charge screening along the polyelectrolyte chain by counter-ions in the solution (i.e., Na^+
284 or Cl^-) suppresses electrostatic attraction between polyelectrolytes of opposite change and decreases
285 the self-repulsion between charges on the same polyelectrolyte, resulting in more coiled, loopy, and

loose structure of the PEM [34]. For PEM membranes, the negative effect of osmotic pressure on the water flux was less than the positive effect of polyelectrolyte swelling, thereby resulting in an overall increase of water flux. After rinsing the NFG and PEM membranes thoroughly with DI water, the water flux was restored to its initial value. This observation indicates that the PDADMAC/PSS multilayer remained stable under high salinity conditions, and the polymer-polymer ion pairs were not discomposed during the swelling process [64]. Miller et al. [65] also demonstrated that the permeability of neutral solutes (glucose, sucrose, and raffinose) for PDADMAC/PSS membranes increased due to membrane swelling. Therefore, we attribute the decreased removal efficiency of divalent cations by PEM membranes under high ionic strength (Figures 5 and 6) also to the swelling of the multilayers that further enhance the permeability of cations.

Figure 6

Figure 7 illustrates the mechanisms underlying the performance of the PDADMAC-terminated PEM membranes under different ionic strengths. Cation removal by the PEM membranes is due to a combined effect of Donnan (charge)- and steric (size)-exclusion mechanisms. The contribution of each mechanism to the overall rejection depends on the interaction between the polyelectrolyte chains and the surrounding ions. At low ionic strength (Figure 7A), the polyelectrolyte chains are relatively stretched due to reduced charge screening of the polyelectrolyte by the surrounding ions, resulting in strong self-repulsion between charges on the same chain as well as intramolecular repulsion between neighboring polymer chains with the same charge [66, 67]. The positive charge of the capping PDADMAC layer provides strong Donnan exclusion of divalent cations, leading to high rejection of divalent cations and high selectivity (Na^+/X^{2+}).

At high ionic strength (Figure 7B), however, the polyelectrolyte charges are effectively screened by the abundant counter-ions (Cl^- or Na^+) present in solution. The charge screening effect weakens the repulsion forces between (i) the capping PDADMAC and cations in solution and (ii) neighboring functional groups carrying the same charge within the polymer chains. While the reduced interactions between PDADMAC and cations directly reduces the Donnan exclusion effect and therefore the cation rejection of the PEM membranes, the weakened intramolecular repulsion within the polymer chains results in the swelling of polyelectrolytes [28, 31]. The loose structure of

the polyelectrolyte layer caused by swelling leads to permeation of both water and salt, resulting in decreased cation rejection and increased water permeability. In addition, the high concentration of counter-ions in solution may cause local folding of the polymer chains and generate large pores that increase salt permeability [66]. Cross-linking of the polyelectrolytes can be used to alleviate the swelling behavior at the expense of reduced water permeability [67]. However, Donnan (charge) exclusion, one of the primary mechanisms for divalent cation removal by PEM membranes, will be still limited by charge screening in high-salinity solutions.

Figure 7

4. Conclusion

Highly selective rejection of divalent cations was achieved with polyelectrolyte multilayer NF membranes fabricated by a simple and convenient layer-by-layer method. The PDADMAC-terminated multilayer membrane exhibited a more positively charged surface than the NFG substrate membrane and PSS-terminated membrane, thus demonstrating a great potential to remove divalent cations (Mg^{2+}, Ca^{2+}, Sr^{2+}, and Ba^{2+}) selectively from feedwaters. The rejection and selectivity (Na^{+}/X^{2+}) are strongly dependent on (i) the number of polyelectrolyte bilayers, (ii) the type of the divalent cation, and (iii) the ionic strength of the feed solution. The number of PEM bilayers affects both Donnan-exclusion and size-exclusion mechanisms. Specifically, PEM membranes with 4.5 and 5.5 bilayers provided adequate positive charge to reject divalent cations effectively, meanwhile maintaining high water and Na^{+} permeabilities. Divalent cations with larger hydrated radius, higher ionic charge density, and greater hydration free energy showed higher rejection by PEM membranes. The ionic strength of the feed solution influences the PEM performance via charge screening and polymer swelling.

Under low ionic strength conditions (e.g., <50 mM NaCl as a background electrolyte), the PEM membranes with 4.5 and 5.5 polyelectrolyte bilayers maintained high rejection of divalent cations. At high ionic strength, the abundant Na^{+} and Cl^{-} ions not only weakened the Donnan exclusion effect by screening the charge of the polyelectrolytes, but also led to swelling of the polymer chains and loosened the structure of the polyelectrolyte multilayer. As a result, cation removal efficiency and selectivity (Na^{+}/X^{2+}) dropped markedly, accompanied by an increase of

water permeability compared to that under low ionic strength conditions. Despite their compromised performance under high ionic strength, these PEM membranes can be used for scaling control by pretreatment of feedwaters with mild-salinity, such as brackish water with <5000 mg/L of total dissolved solids.

Acknowledgments

We acknowledge the support from the National Science Foundation (NSF) Nanosystems Engineering Research Center for Nanotechnology Enabled Water Treatment (Grant EEC-1449500). We also thank for the support from China Scholarship Council (CSC) Graduate Fellowship for C. W.

Appendix A. Supplementary material

Supplementary data associated with this article can be found in the online version.

References

[1] A. Rahardianto, B.C. McCool, Y. Cohen, Reverse osmosis desalting of inland brackish water of high gypsum scaling propensity: kinetics and mitigation of membrane mineral scaling, Environ. Sci. Technol., 42 (2008) 4292-4297.

[2] D.M. Warsinger, J. Swaminathan, E. Guillen-Burrieza, H.A. Arafat, J.H. Lienhard V, Scaling and fouling in membrane distillation for desalination applications: A review, Desalination, 356 (2015) 294-313.

[3] J. Zhang, W.L.C. Loong, S. Chou, C. Tang, R. Wang, A.G. Fane, Membrane biofouling and scaling in forward osmosis membrane bioreactor, J. Membr. Sci., 403-404 (2012) 8-14.

[4] P. Xu, C. Bellona, J.E. Drewes, Fouling of nanofiltration and reverse osmosis membranes during municipal wastewater reclamation: Membrane autopsy results from pilot-scale investigations, J. Membr. Sci., 353 (2010) 111-121.

[5] Y. Le Gouellec, Calcium sulfate (gypsum) scaling in nanofiltration of agricultural drainage water, J. Membr. Sci., 205 (2002) 279-291.

[6] S. Shirazi, C.-J. Lin, D. Chen, Inorganic fouling of pressure-driven membrane processes — A critical review, Desalination, 250 (2010) 236-248.

[7] B. Mi, M. Elimelech, Gypsum scaling and cleaning in forward osmosis: Measurements and mechanisms, Environ. Sci. Technol., 44 (2010) 2022-2028.

[8] D.L. Shaffer, M.E. Tousley, M. Elimelech, Influence of polyamide membrane surface

chemistry on gypsum scaling behavior, J. Membr. Sci., 525 (2017) 249-256.
[9] E. Thompson Brewster, A.J. Ward, C.M. Mehta, J. Radjenovic, D.J. Batstone, Predicting scale formation during electrodialytic nutrient recovery, Water Res. , 110 (2017) 202-210.
[10] M. Xie, S.R. Gray, Gypsum scaling in forward osmosis: Role of membrane surface chemistry, J. Membr. Sci., 513 (2016) 250-259.
[11] W.J. Sang, C.R. Stoof, W. Zhang, V.L. Morales, B. Gao, R.W. Kay, L. Liu, Y.L. Zhang, T.S. Steenhuis, Effect of hydrofracking fluid on colloid transport in the unsaturated zone, Environ. Sci. Technol., 48 (2014) 8266-8274.
[12] N.R. Warner, C.A. Christie, R.B. Jackson, A. Vengosh, Impacts of shale gas wastewater disposal on water quality in western Pennsylvania, Environ. Sci. Technol., 47 (2013) 11849-11857.
[13] D.J. Miller, X.F. Huang, H. Li, S. Kasemset, A. Lee, D. Agnihotri, T. Hayes, D.R. Paul, B.D. Freeman, Fouling-resistant membranes for the treatment of flowback water from hydraulic shale fracturing: A pilot study, J. Membr. Sci., 437 (2013) 265-275.
[14] B.D. Coday, N. Almaraz, T.Y. Cath, Forward osmosis desalination of oil and gas wastewater: Impacts of membrane selection and operating conditions on process performance, J. Membr. Sci., 488 (2015) 40-55.
[15] D. Hasson, A. Drak, R. Semiat, Induction times induced in an RO system by antiscalants delaying CaSO4 precipitation, Desalination, 157 (2003) 193-207.
[16] J.S. Vrouwenvelder, S.A. Manolarakis, H.R. Veenendaal, D. van der Kooij, Biofouling potential of chemicals used for scale control in RO and NF membranes, Desalination, 132 (2000) 1-10.
[17] L. Weinrich, C.N. Haas, M.W. LeChevallier, Recent advances in measuring and modeling reverse osmosis membrane fouling in seawater desalination: a review, J. Water Reuse Desal., 3 (2013) 85.
[18] M. Turek, K. Mitko, K. Piotrowski, P. Dydo, E. Laskowska, A. Jakóbik-Kolon, Prospects for high water recovery membrane desalination, Desalination, 401 (2017) 180-189.
[19] J. Schaep, B. Van der Bruggen, C. Vandecasteele, D. Wilms, Influence of ion size and charge in nanofiltration, Sep. Purif. Technol., 14 (1998) 155-162.
[20] A.W. Mohammad, Y.H. Teow, W.L. Ang, Y.T. Chung, D.L. Oatley-Radcliffe, N. Hilal, Nanofiltration membranes review: Recent advances and future prospects, Desalination, 356 (2015) 226-254.
[21] H. Al-Zoubi, W. Omar, Rejection of salt mixtures from high saline by nanofiltration membranes, Korean J. Chem. Eng., 26 (2009) 799-805.
[22] M. Pontié, H. Dach, J. Leparc, M. Hafsi, A. Lhassani, Novel approach combining physico-chemical characterizations and mass transfer modelling of nanofiltration and low pressure reverse osmosis membranes for brackish water desalination intensification, Desalination, 221 (2008) 174-191.
[23] G.-R. Xu, S.-H. Wang, H.-L. Zhao, S.-B. Wu, J.-M. Xu, L. Li, X.-Y. Liu, Layer-by-layer (LBL) assembly technology as promising strategy for tailoring pressure-driven desalination membranes, J. Membr. Sci., 493 (2015) 428-443.
[24] B.W. Stanton, J.J. Harris, M.D. Miller, M.L. Bruening, Ultrathin, multilayered polyelectrolyte films as nanofiltration membranes, Langmuir, 19 (2003) 7038-7042.
[25] W.Q. Jin, A. Toutianoush, B. Tieke, Use of polyelectrolyte layer-by-layer assemblies as nanofiltration and reverse osmosis membranes, Langmuir, 19 (2003) 2550-2553.
[26] L.Y. Ng, A.W. Mohammad, C.Y. Ng, A review on nanofiltration membrane fabrication

and modification using polyelectrolytes: Effective ways to develop membrane selective barriers and rejection capability, Adv. Colloid Interfa., 197 (2013) 85-107.
[27] J. de Grooth, D.M. Reurink, J. Ploegmakers, W.M. de Vos, K. Nijmeijer, Charged micropollutant removal with hollow fiber nanofiltration membranes based on polycation/polyzwitterion/polyanion multilayers, ACS Appl. Mater. Inte., 6 (2014) 17009-17017.
[28] O.Y. Lu, R. Malaisamy, M.L. Bruening, Multilayer polyelectrolyte films as nanofiltration membranes for separating monovalent and divalent cations, J. Membr. Sci., 310 (2008) 76-84.
[29] S. Rajabzadeh, C. Liu, L. Shi, R. Wang, Preparation of low-pressure water softening hollow fiber membranes by polyelectrolyte deposition with two bilayers, Desalination, 344 (2014) 64-70.
[30] L. Krasemann, B. Tieke, Selective ion transport across self-assembled alternating multilayers of cationic and anionic polyelectrolytes, Langmuir, 16 (2000) 287-290.
[31] A.A. Antipov, G.B. Sukhorukov, H. Möhwald, Influence of the ionic strength on the polyelectrolyte multilayers' permeability, Langmuir, 19 (2003) 2444-2448.
[32] B. Chen, I.A. Meinertzhagen, S.R. Shaw, Circadian rhythms in light-evoked responses of the fly's compound eye, and the effects of neuromodulators 5-HT and the peptide PDF, J. Comp. Physiol. A, 185 (1999) 393-404.
[33] Q. Saren, C.Q. Qiu, C.Y. Tang, Synthesis and characterization of novel forward osmosis membranes based on Layer-by-Layer assembly, Environ. Sci. Technol., 45 (2011) 5201-5208.
[34] N. Joseph, P. Ahmadiannamini, R. Hoogenboom, I.F.J. Vankelecom, Layer-by-layer preparation of polyelectrolyte multilayer membranes for separation, Polym. Chem., 5 (2014) 1817-1831.
[35] Q. Zhao, Q.F. An, Y. Ji, J. Qian, C. Gao, Polyelectrolyte complex membranes for pervaporation, nanofiltration and fuel cell applications, J. Membr. Sci., 379 (2011) 19-45.
[36] S.U. Hong, M.L. Bruening, Separation of amino acid mixtures using multilayer polyelectrolyte nanofiltration membranes, J. Membr. Sci., 280 (2006) 1-5.
[37] C. Cheng, A. Yaroshchuk, M.L. Bruening, Fundamentals of selective ion transport through multilayer polyelectrolyte membranes, Langmuir, 29 (2013) 1885-1892.
[38] A. Tiraferri, M. Elimelech, Direct quantification of negatively charged functional groups on membrane surfaces, J. Membr. Sci., 389 (2012) 499-508.
[39] R. Malaisamy, A. Talla-Nwafo, K.L. Jones, Polyelectrolyte modification of nanofiltration membrane for selective removal of monovalent anions, Sep. Purif. Technol., 77 (2011) 367-374.
[40] O. Sanyal, A.N. Sommerfeld, I. Lee, Design of ultrathin nanostructured polyelectrolyte-based membranes with high perchlorate rejection and high permeability, Sep. Purif. Technol., 145 (2015) 113-119.
[41] R. Epsztein, W. Cheng, E. Shaulsky, N. Dizge, M. Elimelech, Elucidating the mechanisms underlying the difference between chloride and nitrate rejection in nanofiltration, J. Membr. Sci., (2017).
[42] B.N. Dickhaus, R. Priefer, Determination of polyelectrolyte pKa values using surface-to-air tension measurements, Colloids Surf. A, 488 (2016) 15-19.
[43] Y. Lvov, K. Ariga, M. Onda, I. Ichinose, T. Kunitake, A careful examination of the adsorption step in the alternate layer-by-layer assembly of linear polyanion and polycation, Colloids Surf. A, 146 (1999) 337-346.
[44] S.L. Walker, S. Bhattacharjee, E.M.V. Hoek, M. Elimelech, A novel asymmetric clamping cell for measuring streaming potential of flat surfaces, Langmuir, 18 (2002) 2193-2198.

[45] T. Tong, S. Zhao, C. Boo, S.M. Hashmi, M. Elimelech, Relating silica scaling in reverse osmosis to membrane surface properties, Environ. Sci. Technol., 51 (2017) 4396-4406.
[46] E. Shaulsky, S. Nejati, C. Boo, F. Perreault, C.O. Osuji, M. Elimelech, Post-fabrication modification of electrospun nanofiber mats with polymer coating for membrane distillation applications, Environ. Sci. Technol., 530 (2017) 158-165.
[47] R. Epsztein, O. Nir, O. Lahav, M. Green, Selective nitrate removal from groundwater using a hybrid nanofiltration–reverse osmosis filtration scheme, Chem. Eng. J. , 279 (2015) 372-378.
[48] B. Helena, Temporal evolution of groundwater composition in an alluvial aquifer (Pisuerga River, Spain) by principal component analysis, Water Res., 34 (2000) 807-816.
[49] S. Phuntsho, F. Lotfi, S. Hong, D.L. Shaffer, M. Elimelech, H.K. Shon, Membrane scaling and flux decline during fertiliser-drawn forward osmosis desalination of brackish groundwater, Water Res. , 57 (2014) 172-182.
[50] B. Su, T. Wang, Z. Wang, X. Gao, C. Gao, Preparation and performance of dynamic layer-by-layer PDADMAC/PSS nanofiltration membrane, J. Membr. Sci., 423-424 (2012) 324-331.
[51] M. Elzbieciak, M. Kolasinska, P. Warszynski, Characteristics of polyelectrolyte multilayers: The effect of polyion charge on thickness and wetting properties, Colloids Surf. A, 321 (2008) 258-261.
[52] J. de Grooth, R. Oborný, J. Potreck, K. Nijmeijer, W.M. de Vos, The role of ionic strength and odd–even effects on the properties of polyelectrolyte multilayer nanofiltration membranes, J. Membr. Sci., 475 (2015) 311-319.
[53] M. McCormick, R.N. Smith, R. Graf, C.J. Barrett, L. Reven, H.W. Spiess, NMR studies of the effect of adsorbed water on polyelectrolyte multilayer films in the solid state, Macromolecules, 36 (2003) 3616-3625.
[54] E.R. NIGHTINGA, Phenomenological theory of ion solvation. Effective radii of hydrated ions, J. Phys. Chem. C, 63 (1959) 1381-1387.
[55] B. Tansel, J. Sager, T. Rector, J. Garland, R.F. Strayer, L. Levine, M. Roberts, M. Hummerick, J. Bauer, Significance of hydrated radius and hydration shells on ionic permeability during nanofiltration in dead end and cross flow modes, Sep. Purif. Technol., 51 (2006) 40-47.
[56] A.G. Volkov, S. Paula, D.W. Deamer, Two mechanisms of permeation of small neutral molecules and hydrated ions across phospholipid bilayers, Bioelectrochem. Bioenerg., 42 (1997) 153-160.
[57] A. Alarifi, H.A. Hanafi, Adsorption of cesium, thallium, strontium and cobalt radionuclides using activated carbon, J. Atom. Mol. Sci., 1 (2010) 292-300.
[58] Y. Marcus, A simple empirical model describing the thermodynamics of hydration of ions of widely varying charges, sizes, and shapes, Biophys. Chem. , 51 (1994) 111-127.
[59] D.-X. Wang, M. Su, Z.-Y. Yu, X.-L. Wang, M. Ando, T. Shintani, Separation performance of a nanofiltration membrane influenced by species and concentration of ions, Desalination, 175 (2005) 219-225.
[60] R. Epsztein, E. Shaulsky, N. Dizge, Y. Roy, D.M. Warsinger, M. Elimelech, Ionic charge densitiy-dependent Donnan exclusion in nanofiltration of monovalent anions, Environ. Sci. Technol., under review.
[61] L.A. Richards, A.I. Schäfer, B.S. Richards, B. Corry, The importance of dehydration in determining ion transport in narrow pores, Small, 8 (2012) 1701-1709.
[62] M.A. Alghoul, P. Poovanaesvaran, K. Sopian, M.Y. Sulaiman, Review of brackish water

reverse osmosis (BWRO) system designs, Renew. Sust. Energ. Rev., 13 (2009) 2661-2667.
[63] J. Luo, Y. Wan, Effect of highly concentrated salt on retention of organic solutes by nanofiltration polymeric membranes, J. Membr. Sci., 372 (2011) 145-153.
[64] S.T. Dubas, J.B. Schlenoff, Polyelectrolyte multilayers containing a weak polyacid: Construction and deconstruction, Macromolecules, 34 (2001) 3736-3740.
[65] M.D. Miller, M.L. Bruening, Correlation of the swelling and permeability of polyelectrolyte multilayer films, Chem Mater, 17 (2005) 5375-5381.
[66] G.S. Manning, Is the counterion condensation point on polyelectrolytes a trigger of structural transition?, J. Chem. Phys., 89 (1988) 3772-3777.
[67] A.M. Mika, R.F. Childs, J.M. Dickson, B.E. McCarry, D.R. Gagnon, Porous, polyelectrolyte-filled membranes: Effect of cross-linking on flux and separation, J. Membr. Sci., 135 (1997) 81-92.
[68] H. Binder, O. Zschörnig, The effect of metal cations on the phase behavior and hydration characteristics of phospholipid membranes, Chem. Phys. Lipids 115 (2002) 39-61.

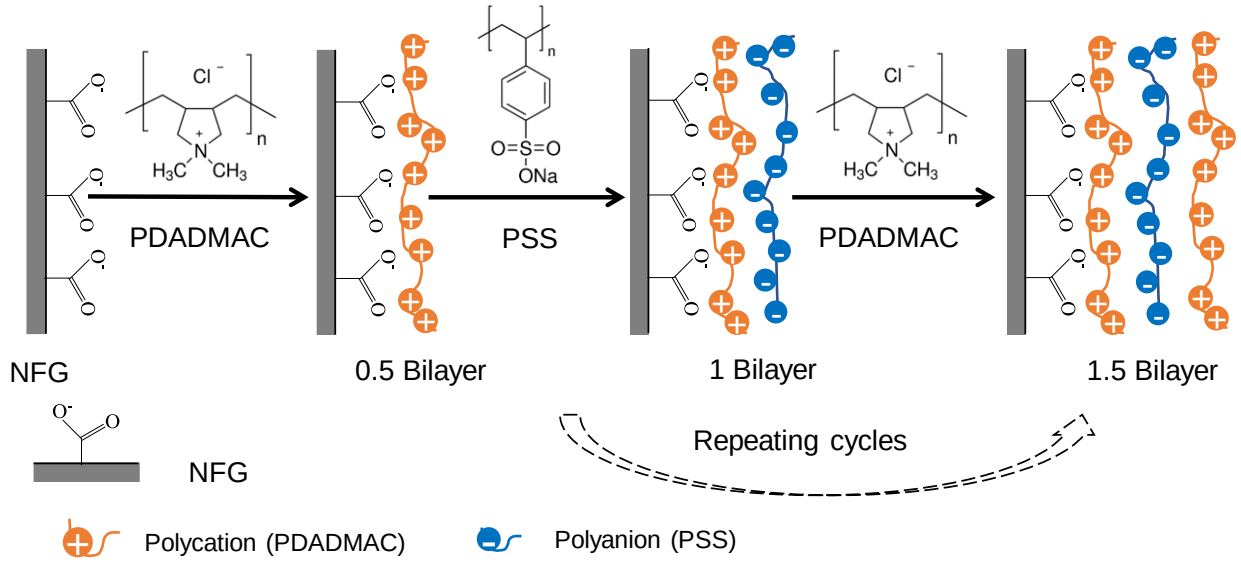

Fig. 1. Schematic of multilayer polyelectrolyte membranes fabrication with alternating electrostatic deposition of polycation (poly(diallyldimethylammonium chloride), PDADMAC) and polyanion ((poly(sodium 4-styrenesulfonate), PSS) on NFG substrate. The schematic was adopted from reference [27].

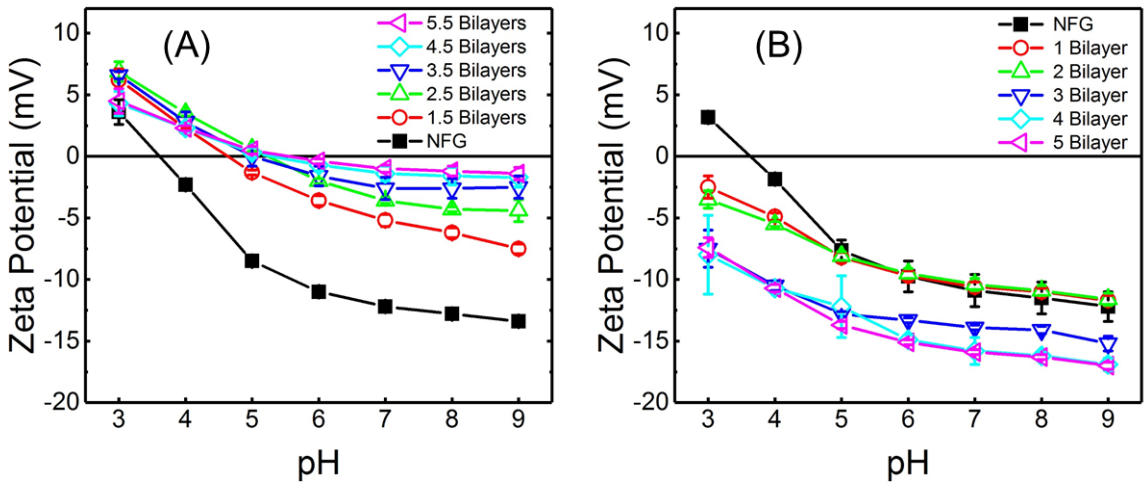

Fig. 2. Zeta potential of (A) PDADMAC polymer terminated membranes and (B) PSS polymer terminated membranes as a function of pH. The error bars represent standard deviation and were calculated from duplicate measurements.

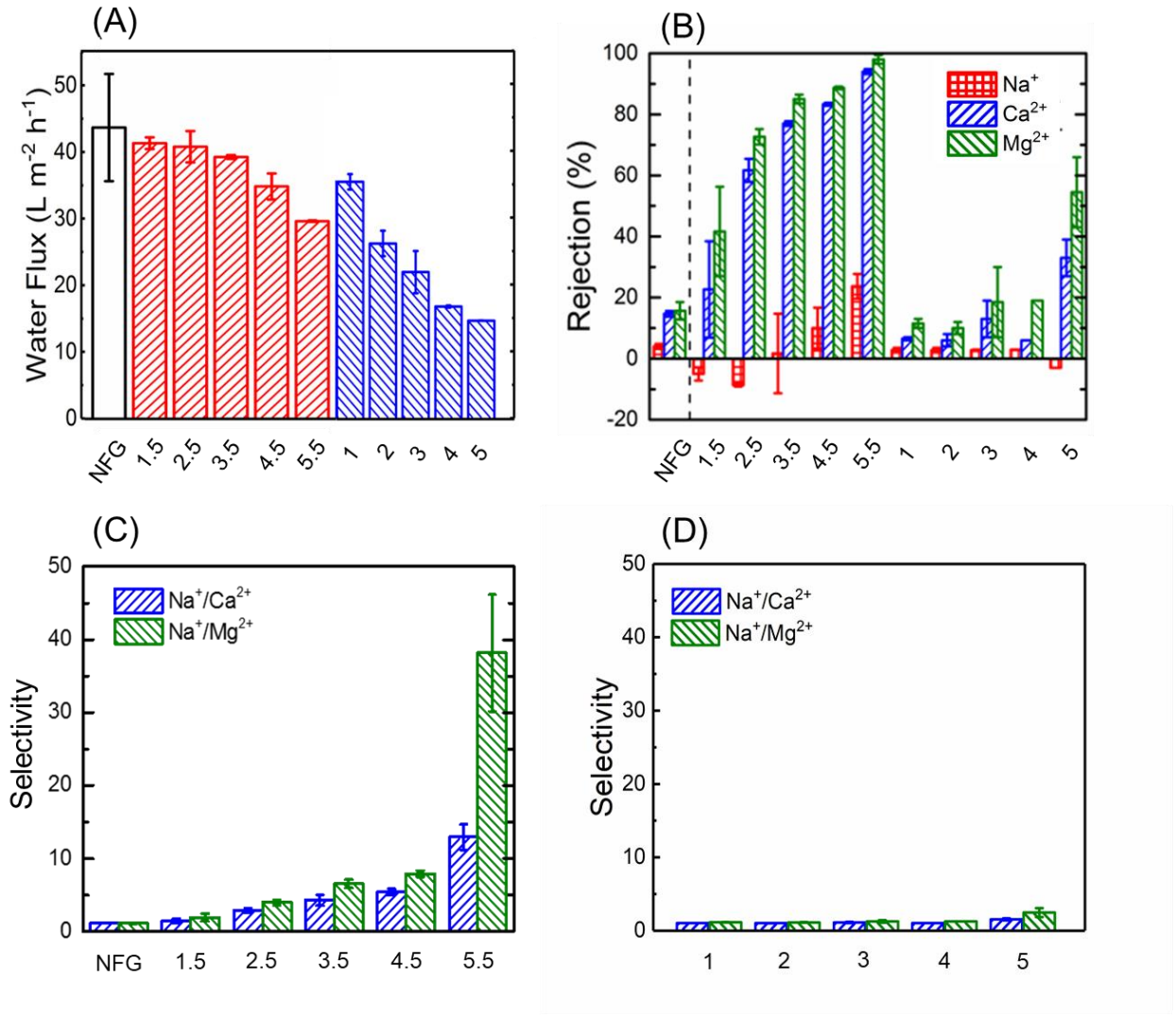

Fig. 3. Permeability and selectivity of polyelectrolyte NF membranes with different bilayer numbers and surface charge. Membranes denoted by "0.5" bilayer were terminated by polycation (PDADMAC), whereas those denoted by integral bilayer were terminated by polyanion (PSS). (A) Water permeability of NFG membrane (white column), positively (red columns) and negatively (blue columns) charged membranes. (B) Rejection of different cations from a feedwater containing 1 mM $CaCl_2$, 1 mM $MgCl_2$ and 5 mM NaCl. The selectivity of sodium ions over divalent cations (Ca^{2+}/Na^+, Mg^{2+}/Na^+) were calculated for (C) positively charged membranes and (D) negatively charged membranes.

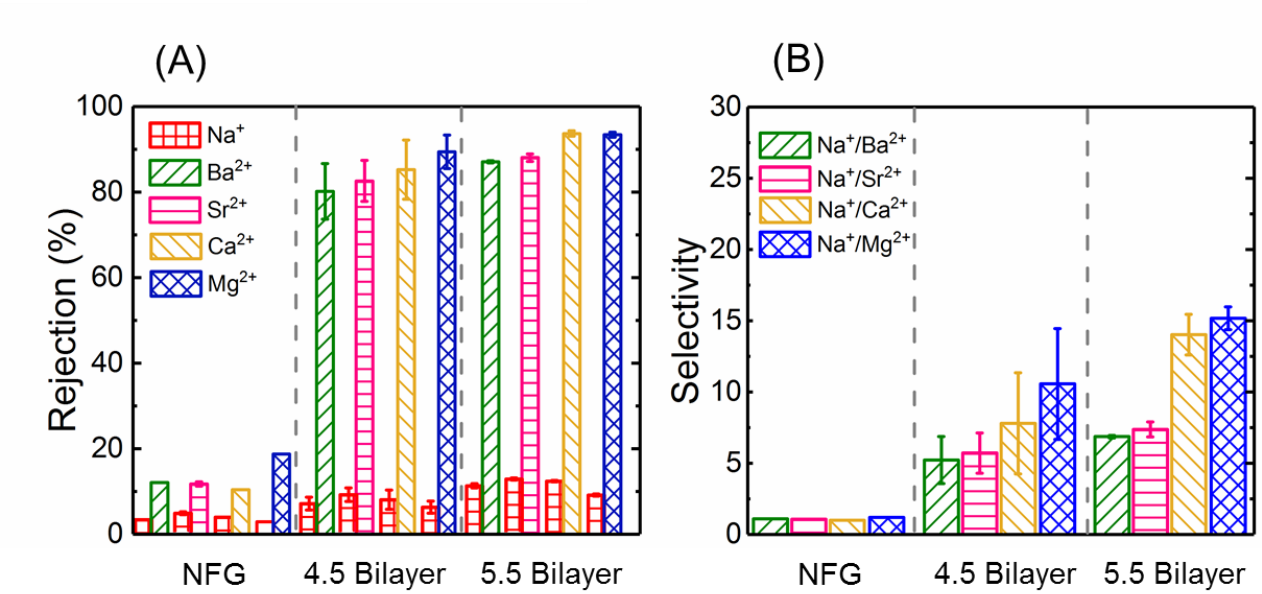

Fig. 4. The rejection of divalent cations and their selectivity (Na^+/X^{2+}) for 4.5- and 5.5- bilayers polyelectrolyte NF membranes. The NFG pristine membrane was used as the control. (A) Cation rejection for mixed salt solution. The feed solution is composed of 5 mM NaCl *and* 1 mM divalent cation salt ($BaCl_2$, $SrCl_2$, $CaCl_2$ or $MgCl_2$). (B) The selectivity of a sodium ion over divalent cations.

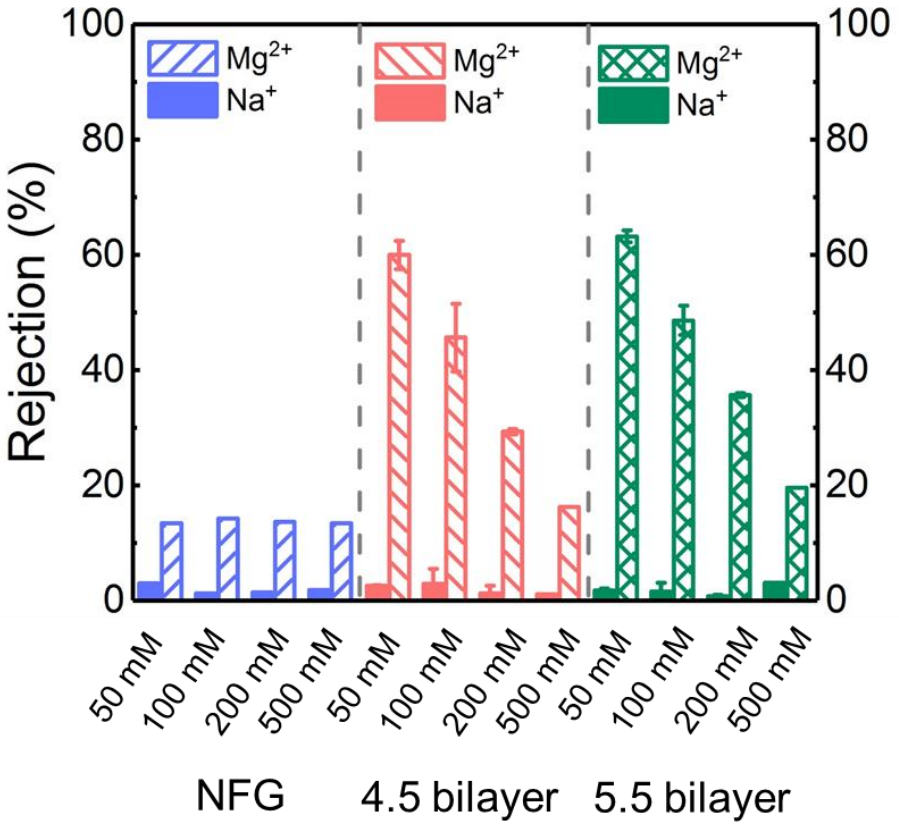

Fig. 5. The rejection of Mg^{2+} as a function of solution ionic strength. The performance of 4.5 bilayers (red) and 5.5 bilayers (green) polyelectrolyte membranes was tested and compared with NFG pristine membrane (blue). Different concentrations of NaCl (50 mM, 100 mM, 200 mM and 500 mM) were used to generate different ionic strengths. The concentration of $MgCl_2$ was 5 mM in all experiments.

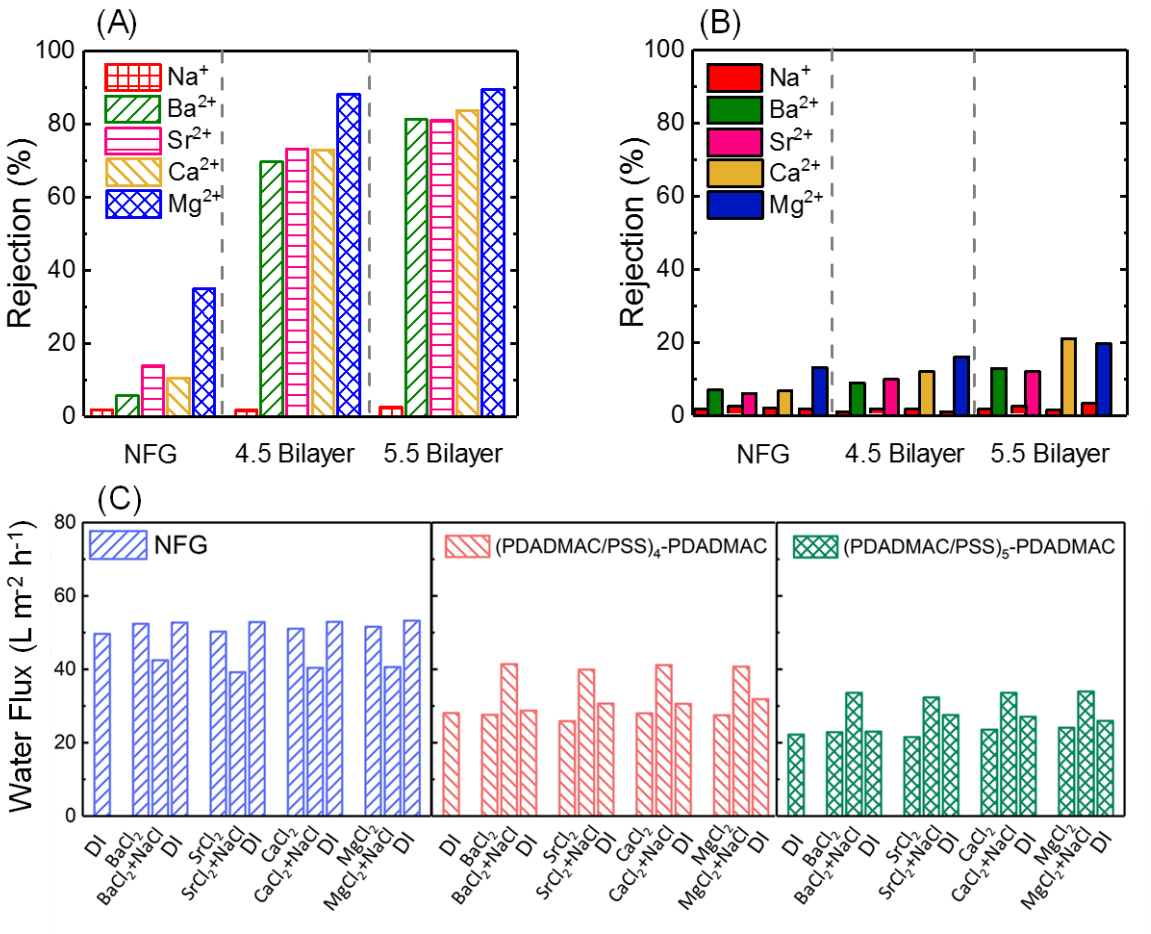

Fig. 6. Divalent cation rejection and water flux under high salinity. (A) The rejection of individual cations, Na^+ (red), Ba^{2+} (green), Sr^{2+} (pink), Ca^{2+} (orange), or Mg^{2+} (blue) at the concentration of 5 mM. (B) The rejection of cations from mixed salt solutions containing both 500 mM NaCl and 5 mM of each divalent salt ($BaCl_2$, $SrCl_2$, $CaCl_2$, or $MgCl_2$). (C) The effects of salinity on water permeability of each membrane. The membranes were subjected to individual and mixed salt solution in sequence, after which physical cleaning with DI water (at 21.37 cm/s cross-flow velocity) was conducted. Then the DI water flux was measured as compared with that prior to salt rejection tests. NFG, 4.5 bilayer and 5.5 bilayer polyelectrolyte membranes were tested in the experiment.

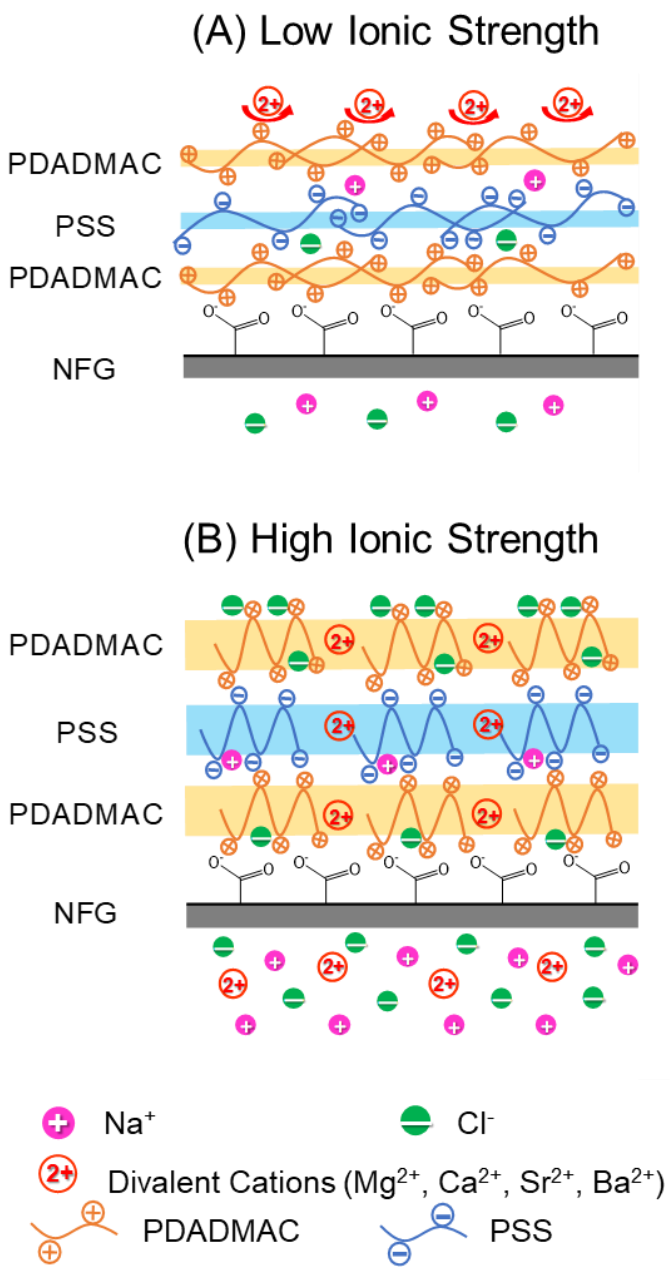

Fig. 7. Schematic of cation transport in PDADMAC-terminated multilayer polyelectrolyte membranes under low (A) and high (B) salinity. Sphere symbols represent monovalent (Pink: Na^+, Green: Cl^-) and divalent (Red: Mg^{2+}, Ca^{2+}, Sr^{2+} and Ba^{2+}) ions. Orange chains and layers represented the PDADMAC polymer and positively charged polyelectrolyte layers. Blue chains and layers represented the PSS polymer and negatively charged polyelectrolyte layers. NFG is a TFC NF membrane used as the substrate of the polyelectrolyte membrane. Note that high salinity results in charge screening and polymer swelling, which influence the transport of both water and cation molecules.

589

590 **Table 1** Hydrated radius, ionic radius and hydration-free energy of the cations.

Cation	Hydrated Radius (nm)[a]	Ionic Radius (nm)[b]	Hydration Free Energy (KJ mol^{-1})[b]
Na^{+}	0.358	0.102	364
Ba^{2+}	0.404	0.136	1249
Sr^{2+}	0.412	0.125	1379
Ca^{2+}	0.412	0.100	1504
Mg^{2+}	0.428	0.072	1828

591 [a] The hydrated radius of the cation was obtained from Nightinga et al.[54]

592 [b] The ionic radius and the hydration-free energy were obtained from Binder et al.[68]

593